CHARACTERIZATION OF THE WELDING ZONE IN STAINLESS STEELS USED IN CSP PLANTS UNDER STATIC CORROSION CONDITIONS WITH MOLTEN SALTS

Abdiel Mallco Carpio[1,2], Mauricio Lague[1], Víctor Vergara[1] and Grover Viracochea[1,2]

[1] Universidad de Antofagasta, Antofagasta (Chile)

[2] Solar Energy Research Center, Santiago (Chile)

Abstract

This study characterizes the corrosion of welded AISI 304 stainless steels, used in Concentrated Solar Power (CSP) plants, when exposed to molten solar salts (60% $NaNO_3$, 40% KNO_3). The research addresses the need to understand corrosion in welded areas, a critical area often overlooked compared to the base metal. Samples were subjected to static corrosion testing in the salt mixture at 550 °C for 1,350 hours. Gravimetric analysis revealed a multiphase corrosion process. Initially, a protective passive layer formed, but after approximately 650 hours, this layer began to degrade, initiating localized corrosion. In advanced stages (>1160 hours), the heat-affected zone (HAZ) was confirmed to be sensitized by the precipitation of chromium carbides ($Cr_{23}C_6$), leading to severe intergranular attack. This research clarifies the time-dependent degradation mechanisms in welded joints, highlighting the synergy between pitting and intergranular corrosion as the main failure mechanism.

Keywords: Static Corrosion, Gravimetric Analysis, Weld Zone, CSP, Sensitization, Intergranular Corrosion.

1. Introduction

It is imperative that the global transition to sustainable energy sources be prioritized to mitigate the effects of climate change, which are largely driven by greenhouse gas (GHG) emissions from fossil fuels. In this context, Concentrated Solar Power (CSP) emerges as a promising technology for its ability to generate electricity on a large scale. It also integrates well with Thermal Energy Storage (TES) systems, which enable dispatchable and continuous power generation [4-5-7]. This is an advantage over other renewables, such as photovoltaics (PV), which are subject to intermittency. TES systems in commercial CSP plants, such as central tower and parabolic trough collectors, primarily utilize a eutectic mixture of molten salts, known as solar salt (60% by weight $NaNO_3$ and 40% by weight KNO_3), as a heat transfer and storage fluid [1-6].

This medium operates in a temperature range of up to 565 °C. However, its high chemical aggression at high temperatures poses significant corrosion challenges for structural components in the plant, such as pipes, tanks, and pumps. Austenitic stainless steel AISI 304 is a structural material that is frequently used in these applications due to its favorable cost-performance ratio [8-9]. While it offers adequate corrosion resistance in nitrate salts up to approximately 565 °C, its performance can be compromised, especially in welded joints. Welding is an indispensable manufacturing process, but it locally alters the microstructure of the material, creating a weld zone (WZ), a heat-affected zone (HAZ), and the base metal (BM), each with different susceptibility to corrosion [2-3-10].

The central problem of this research lies in sensitization, a microstructural degradation phenomenon that affects austenitic stainless steels when exposed to temperatures between 450 °C and 900 °C. The experimental temperature of this study, 550 °C, falls within this critical range. Sensitization involves the precipitation of chromium carbides (mainly $Cr_{23}C_6$) at grain boundaries. This process consumes chromium from adjacent areas, creating chromium-depleted zones that are highly vulnerable to intergranular corrosion (IGC), a phenomenon often referred to as "weld decay." Since the diffusion processes governing carbide formation are thermally activated, at 550°C the sensitization kinetics are expected to be relatively slow [3].

10.18086/swc.2025.01.04 Available at http://proceedings.ises.org

This suggests that IGC will not be an immediate failure mode, but rather a long-term degradation mechanism, whose onset and progression are crucial for predicting the service life of components [3].

Although uniform corrosion of the base metal has been extensively studied, there is a lack of understanding of the temporal evolution of corrosion mechanisms in AISI 304 welded joints under realistic CSP operating conditions. Therefore, the objective of this work is to characterize the corrosion kinetics and microstructural degradation of AISI 304 welded joints in molten solar salt, with a specific focus on identifying the initiation, progression, and impact of sensitization and localized attack.

2. Experimental Procedure

2.1. Materials and Welding Process

For this study, AISI 304 austenitic stainless-steel tubes with an outer diameter of 101.6 mm and a wall thickness of 2 mm were used. The chemical composition of the material was determined by optical emission spectroscopy and is shown in Table 1. The carbon content of 0.069% by weight is significantly higher than the threshold for low carbon "L" grades (<0.03%), confirming the inherent susceptibility of the material to sensitization.

Table 1: Elemental composition (% by weight) of the AISI 304 stainless steel used.

% by weight	C	Mn	S	Si	Cr	Ni	Others
AISI 304 sample	0.069	0.886	0.037	0.528	18.63	7.584	Fe: Balance

The welding process utilized a tungsten inert gas (TIG) method with pulsed direct current, excluding the use of filler material. The key welding parameters are detailed in

Table 2. Argon gas was used as a shielding gas to protect the root of the weld.

Parameter	Unit	Values
Pulse current	A	81
Base current	A	30
Pulse time	Ms	149
Base time	Ms	260
Welding speed	mm/min	85
Electrode tip angle	°	15
Arc length	Mm	1.8
Polarity	Direct	

2.2. Corrosion Test Methodology

A eutectic mixture of solar salt was prepared, composed of 60% by weight of $NaNO_3$ (99.5% purity) and 40% by weight of KNO_3 (99.28% purity). The welded tubes were cut into 10 x 10 mm test pieces, with the weld bead centered on each sample. The test pieces were immersed in alumina crucibles containing the salt and kept in an oven at a constant temperature of 550 °C in static air for a total time of 1,350 hours. Samples were collected at predetermined intervals for analysis.

3. Gravimetric and Microstructural Analysis

The corrosion kinetics were evaluated using gravimetric analysis, which involved measuring the mass gain per unit area at each time interval. The mass gain was calculated using Equation 1, where m_f is the final mass, m_i is the initial mass, and S_0 is the initial surface area of the sample.

$$\frac{\Delta m}{S_0} = \frac{m_f - m_i}{S_0} \quad (1)$$

Following each exposure period, the samples were meticulously cleaned to ensure the removal of any salt residues. The following techniques were used for post-exposure characterization: The following procedures were used to obtain the desired results: Scanning Electron Microscopy (SEM) with Energy Dispersive X-ray Spectroscopy (EDS) was used for morphological and elemental analysis. X-ray Diffraction (XRD) was used to identify corrosion product phases. Optical Microscopy of cross sections electrochemically etched with oxalic acid was used to reveal microstructure, grain boundaries, and sensitization characteristics.

4. Results and Discussion

4.1. Corrosion Kinetics and Gravimetric Analysis

Figure 1 illustrates the progression of mass accumulation in welded AISI 304 specimens as a function of exposure duration. The curve reveals nonlinear and complex corrosion behavior, which can be divided into several stages, reflecting a progressive transition of degradation mechanisms.

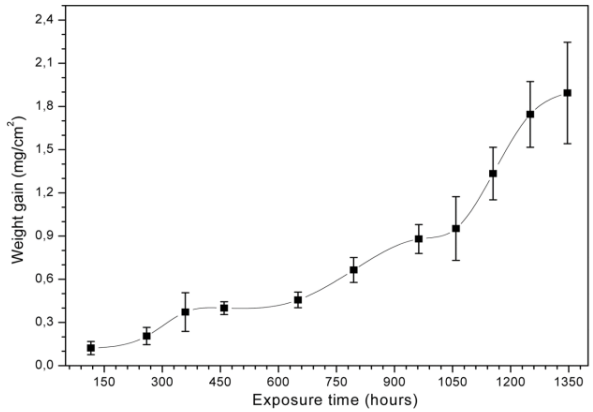

Figure 1. This figure illustrates the gravimetric evolution of welded AISI 304 stainless steel that was exposed to solar salt at 550°C under static conditions for up to 1,350 hours.

- Stage I (0–360 hours): It is observed that there is rapid initial mass gain, which slows down until it reaches a plateau. This behavior is indicative of the formation of an initial oxide layer, which offers partial protection, thereby limiting the subsequent corrosion rate.
- Stage II (360–650 hours): The rate of mass gain stabilizes, forming a first plateau. This suggests that the oxide layer formed is temporarily passivating and controls the interaction between the metal and the molten salt.
- Stage III (650–950 h): After 650 hours, there is a significant increase in mass gain. This critical turning point indicates the breakdown of the initial passive layer and the onset of more aggressive and localized corrosion mechanisms.
- Stages IV and V (950–1350 h): Following a brief second plateau from 950 to 1050 hours, the corrosion rate experiences a significant increase. This final phase corresponds to advanced degradation, where the oxide layer completely loses its integrity and severe failure mechanisms are activated.

It is imperative to interpret this gravimetric curve with caution. This measurement indicates an average mass gain over the entire surface of the sample. However, microstructural analysis reveals that corrosion damage is not uniform but rather concentrated intensely in the weld and HAZ regions, which constitute a small fraction of the total area. Therefore, the curve does not reflect an overall acceleration of corrosion, but rather the initiation and propagation of localized, severe attack in these vulnerable areas. The inflection point at 650 hours indicates the transition when localized corrosion at the welded joint becomes the predominant factor

driving total mass gain. Relying solely on gravimetric analysis may underestimate the severity of localized damage, which will ultimately dictate the service life of the component.

5. Microstructural and Morphological Evolution

A chronological analysis of the microstructure and surface morphology reveals the sequence of degradation events underlying the gravimetric curve. Figure 2 presents a compilation of micrographs illustrating the key stages of this process.

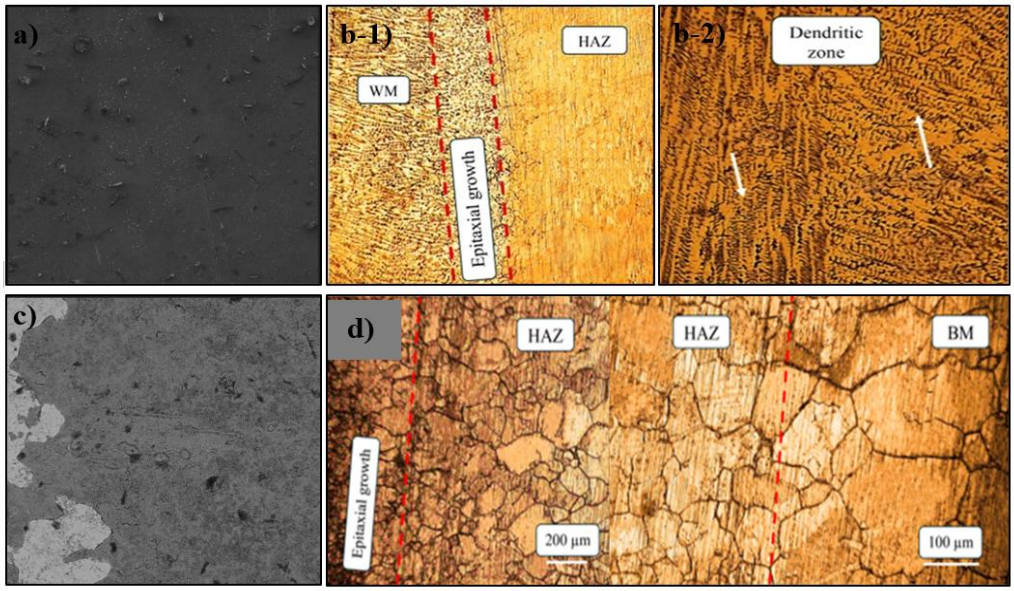

Figure 2: Microstructural evolution of the AISI 304 welded joint. (a) SEM surface at 360 h showing a continuous oxide layer. (b) Optical micrograph of the cross section at 360 h with no visible attack. (c) SEM image of the surface at 960 h showing pitting and porosity. (d) Optical micrograph of the HAZ at 1350 h showing a continuous network of intergranular precipitates (sensitization).

Initial Stage (0–360 hours): The Formation of a Protective Oxide Layer

In the initial 360 hours, SEM images demonstrate a continuous and adherent oxide layer, with no indications of cracks, delamination, or pitting. XRD analysis identified the primary crystalline phases as magnetite (Fe_3O_4) and an iron-chromium spinel ($FeCr_2O_4$), which is consistent with the formation of a passive layer on stainless steels in molten nitrates. Optical micrographs of the sections confirmed the integrity of the grain boundaries in the MB, SZ, and HAZ, with no evidence of intergranular attack. This behavior aligns with the initial plateau of the gravimetric curve, suggesting a transient passivation phase.

Intermediate Stage (650–960 hours): Localized Corrosion

After 650 hours, there is a significant change in the corrosion behavior. SEM images of the surface at 960 h reveal the appearance of pitting, porous oxide structures, and increased surface roughness. Damage begins in the SZ and HAZ, where microstructural heterogeneities (dendritic structures, residual stresses) act as nucleation sites for the passive layer breakdown. XRD analysis during this period indicates an increase in the intensity of hematite (Fe_2O_3) peaks, a less protective oxide, confirming the loss of barrier integrity. This morphological change corresponds with the re-acceleration of mass gain that was observed after 650 hours.

Advanced Stage (1160–1350 h): Sensitization and Intergranular Attack

In the final phase of exposure, sensitization becomes the predominant degradation mechanism. XRD analysis at 1160 and 1350 hours provides definitive evidence, showing the appearance of new diffraction peaks corresponding to $Cr_{23}C_6$ type chromium carbides. Concurrently, high-magnification optical micrographs of the attacked HAZ demonstrate a continuous, well-defined network of precipitates along the grain boundaries. This is the classic microstructural signature of sensitization, which creates low-resistance corrosion pathways. This

severe microstructural degradation directly correlates with the final, catastrophic acceleration of mass gain, as the molten salt can now preferentially attack these chromium-depleted zones.

5.1. Proposed Time-Dependent Corrosion Mechanism

According to the findings of our experimental study, we can propose a three-stage corrosion mechanism that describes the progressive degradation of the AISI 304 welded joint.

Stage I - Passivation (0–650 hours): Initially, corrosion is controlled by the formation of a double-layer oxide layer, composed of an inner layer rich in chromium ($FeCr_2O_4$ spinel) and an outer layer of iron oxide (Fe_3O_4). This layer functions as a diffusion barrier, thereby maintaining a low corrosion rate.

Stage II - Localized Breakdown (650–1160 h): Microstructural heterogeneities and residual stresses present in the welded joint can lead to the localized breakdown of the passive film. This process initiates pitting corrosion, which penetrates the protective layer and exposes the underlying metal directly to the aggressive molten salt.

Stage III - Synergistic Degradation (>1160 h): As pitting corrosion progresses, prolonged thermal exposure at 550 °C simultaneously causes sensitization of the microstructure in the HAZ. At this point, the two degradation mechanisms act synergistically. The pits that form in the HAZ act as conduits, providing the molten salt with direct access to the newly sensitized and chromium-depleted grain boundaries. This triggers rapid intergranular corrosion, which propagates through the grain boundary network, leading to catastrophic acceleration of material loss and compromising the structural integrity of the component. This synergistic mechanism, where pitting acts as a precursor that “unlocks” intergranular attack, represents the primary failure pathway for these components in service.

6. Conclusions

Research into the corrosion behavior of AISI 304 stainless steel welded joints in molten solar salt at 550 °C has led to the following conclusions: The corrosion process is a multiphase, time-dependent phenomenon that evolves from initial passivation to severe degradation. However, it is important to note that gravimetric analysis alone is not sufficient to accurately assess the severity of the damage, as corrosion tends to occur in the weld zone and HAZ. The initial passive layer's breakdown typically occurs after approximately 650 hours, manifesting as pitting corrosion. This event marks a critical transition to more aggressive corrosion regimes. The final and most critical failure mechanism is HAZ sensitization, confirmed by the detection of chromium carbide ($Cr_{23}C_6$) precipitates after approximately 1160 hours. The extended incubation period for sensitization is attributable to the reduced diffusion kinetics at the test temperature of 550°C. A proposed synergistic failure mechanism involves pitting corrosion acting as a precursor to intergranular attack. The pits provide a pathway for molten salt to access and attack the sensitized grain boundaries, leading to rapid acceleration of material degradation.

Acknowledgements

The authors would like to thank the National Research and Development Agency (ANID) for its financial support, ANID/FONDAP/1523A0006 “Solar Energy Research Center - SERC-Chile.” F. Pineda acknowledges the financial support of ANID-Chile within the projects Fondecyt Regular 1241151 and Fondecyt de Exploración 13240066.

References

[1] Caraballo, A., Galán-Casado, S., Caballero, Á., Serena, S., 2021. Molten salts for sensible thermal energy storage: A review and an energy performance analysis. Energies 14(4), 1197.

[2] Devendranath Ramkumar, K., Pavan, B., Chandrasekar, V., 2018. Development of improved microstructural traits and mechanical integrity of stabilized stainless-steel joints of AISI 321. J Manuf Process 32, 582–594.

[3] García, C., Martín, F., Tiedra, P. de, Aparicio, M.L., 2003. An intergranular corrosion study of welded joints of austenitic stainless steels (AISI 304 and 316L) has been addressed. Corrosion Science 45(8), 1845-1856.

[4] IEA (International Energy Agency), 2022. World Energy Outlook 2022. International Energy Agency, Paris.

[5] IEA (International Energy Agency), 2024. Energy Technology Perspectives 2023. International Energy Agency, Paris.

[6] Li, H., Feng, X., Wang, X., Yang, X., Tang, J., Gong, J., 2022. Impact of temperature on corrosion behavior of austenitic stainless steels in solar salt for CSP application: An electrochemical study. Solar Energy Materials and Solar Cells 239, 111661.

[7] Schlipf, D., Stepper, R., Schneider, G., 2014. CSP Storage Technology - State of the art. Deutsche G. Bonn.

[8] SSINA, 2018. Intergranular Corrosion of Austenitic Stainless Steels. Stainless Steel Information Center.

[9] Thermal Processing, 2023. Intergranular Corrosion of Austenitic Stainless Steels. Thermal Processing Magazine.

[10] Vilchez, F., Pineda, F., Walczak, M., Ramos-Grez, J., 2020. The effect of laser surface melting of stainless steel grade AISI 316L welded joint on its corrosion performance in molten Solar Salt. Solar Energy Materials and Solar Cells 213, 110576.